Deep-Sea Research, 1975, Vol. 22, pp. 583 to 596. Pergamon Press. Printed in Great Britain.

Spin-up of a stratified ocean, with applications to upwelling

DAVID L. T. ANDERSON* and A. E. GILL*

(*Received* 17 *June* 1974; *in revised form* 7 *November* 1974; *accepted* 12 *November* 1974)

Abstract—The method by which an ocean, initially stratified but motionless, adjusts to a suddenly applied wind stress is examined. For wind stress in the east–west direction, the zonal velocity in the ocean interior builds up linearly with time until a long planetary wave arrives from the eastern boundary. Then the interior flow stops increasing and oscillates about a steady value. At the west, a boundary layer forms and gets progressively thinner. The rate of thinning of this boundary layer is reduced by the arrival of long planetary waves from the east but is not stopped. A comparison is made between the barotropic and baroclinic responses.

A comparison is also made between the upwelling at the eastern boundary induced by a longshore wind stress when there are no planetary waves (f-plane) and when there are planetary waves (β-plane). In the former, upwelling is restricted to within a distance of $\sim$ 30 km of the coast, whereas when planetary waves are included the width of the upwelling zone increases with time. On both f- and β-plane, Kelvin waves carry energy poleward along the eastern boundary. For a wind stress which varies sinusoidally with y this results in the mean upwelling being nearly 90° out of phase with the wind stress. The amplitude of the Kelvin wave is damped on the β-plane but suffers no attenuation on the f-plane. The difference between the results for coastal upwelling on an f-plane and that on a β-plane increases as the north–south scale of the forcing is increased. In the case where the scale is infinite, the f-plane upwelling increases indefinitely with time whereas the β-plane solution attains a steady value.

1. INTRODUCTION

This paper seeks to give some insight into the role planetary waves play in the spin-up of the ocean. The questions we seek to answer are (i) how an ocean, initially stratified but at rest, would respond if a steady wind stress were suddenly applied, and (ii) in what way would the barotropic and first baroclinic modes respond differently.

PEDLOSKY (1965a, b, 1967), PHILLIPS (1966), and VERONIS (1963, 1966, 1970) have discussed the response to a wind stress periodic in time, GATES (1968) has considered aspects of the mid-latitude barotropic spin-up problem, and LIGHTHILL (1969, 1971) has considered the effects on the barotropic flow near a western boundary of applying a steady wind stress in low latitudes. Despite the fact that various aspects of boundary effects, stratification, and variation of Coriolis parameter with latitude have been considered, a unified treatment does not appear to exist. Since the ocean spin-up can be summed up rather simply in terms of planetary waves it appears worthwhile to present the results. The model used is formulated in Sections 2–5, and the results for an east–west wind stress are discussed in Sections 6–8.

The oceanic response to an applied north–south wind stress is also of interest, because this form of forcing is very efficient at generating upwelling, an important eastern boundary phenomenon. ICHIYE (1972) and HURLBURT and THOMSON (1973) have considered β effects on upwelling near an eastern boundary, but in the latter formulation the calculations are only performed long enough for the barotropic mode to respond to β dynamics. The inclusion of β effects allows planetary waves to carry the upwelling westward and this implies that upwelling can only attain a certain maximum value, even when the wind stress has an infinite north–

*Department of Applied Mathematics and Theoretical Physics, University of Cambridge, Silver Street, Cambridge CB3 9EW, England.

south length scale. This aspect of the problem is considered in Sections 9 and 10.

2. THE BASIC EQUATIONS

The position of a point in the ocean can be defined by co-ordinates (λ, θ, z) where λ is the longitude (positive eastwards), θ the latitude (positive northwards) and z is distance upwards. Let (u, v, w) be the corresponding velocity components. For small perturbations on a basic state where density surfaces, and the ocean floor, are horizontal, the vertical structure can be described in terms of normal modes (LIGHTHILL, 1969), each of which behaves independently. For a given mode, the equations satisfied by the perturbation are

$$u_t - 2\Omega \sin\theta\, v = -\frac{1}{R}\sec\theta\, p_\lambda + \tau^x/H \tag{2.1}$$

$$v_t + 2\,\Omega \sin\theta\, u = -\frac{1}{R} p_\theta + \tau^y/H \tag{2.2}$$

$$p_t + \frac{c^2}{R}\sec\theta\left[u_\lambda + (v\cos\theta)_\theta\right] = 0, \tag{2.3}$$

where p is the perturbation pressure divided be the density, (τ^x, τ^y) is the wind stress at the surface divided by the density and R is the radius of the Earth. The constants H and c depend on the mode in question; c is the speed of long internal waves for the mode concerned, and H is a measure of the degree of forcing of that mode. In particular, for an ocean consisting of two layers of density ρ_i and depth H_i in which the horizontal velocity is (u_i, v_i) $(i = 1, 2$ for upper and lower layers, respectively) there are two modes. For the barotropic mode one has, to a good approximation

$$u = \frac{H_1u_1 + H_2u_2}{H_1 + H_2};\ p = g\eta;\ H = H_1 + H_2;$$
$$c^2 = gH, \tag{2.4}$$

where g is the acceleration due to gravity and η is the surface elevation. For the baroclinic mode, the approximate values are

$$u = u_1 - u_2;\ p = g'h;\ H = \frac{H_1H_2}{H_1 + H_2};$$
$$c^2 = g'H, \tag{2.5}$$

where h is the elevation of the interface and

$$g' = (\rho_2 - \rho_1)g/\rho_2. \tag{2.6}$$

For the barotropic mode c is about 200 m s^{-1}, while for the baroclinic mode c is about 2 m s^{-1}.

3. AN APPROXIMATION WHICH FILTERS OUT INERTIAL PERIOD MOTIONS

The aim here is to describe adjustments which take place on time scales large compared with the inertial time scale $(2\Omega \sin\theta)^{-1}$. Thus, approximations which ignore $\partial/\partial t$ in comparison with $2\Omega \sin\theta$ seem justified. To obtain such an approximation, consider $\partial/\partial t$ of (2.1) plus $2\Omega \sin\theta$ times (2.2) and $\partial/\partial t$ of (2.2) minus $2\Omega \sin\theta$ times (2.1), i.e.

$$u_{tt} + (2\Omega \sin\theta)^2 u = -\frac{2\Omega}{R}\sin\theta\, p_\theta -$$
$$-\frac{\sec\theta}{R} p_{\lambda t} + \left(2\Omega \sin\theta\, \tau^y + \tau^x_t\right)/H$$

$$v_{tt} + (2\Omega \sin\theta)^2 v = \frac{2\Omega}{R}\sin\theta \sec\theta\, p_\lambda -$$
$$-\frac{1}{R} p_{\theta t} + \left(-2\Omega \sin\theta\, \tau^x + \tau^y_t\right)/H.$$

Assuming that τ^x and τ^y are of the same order, the desired approximation is

$$2\Omega \sin\theta\, u = -\frac{p_\theta}{R} - \frac{\sec\theta}{2\Omega R \sin\theta} p_{\lambda t} + \tau^y/H \tag{3.1}$$

$$2\Omega \sin\theta\, v = \sec\theta\, p_\lambda/R - \frac{1}{2\Omega R \sin\theta} p_{\theta t} -$$
$$-\tau^x/H. \tag{3.2}$$

In much of the ocean, the first term dominates the right-hand side, i.e. there is a geostrophic

balance. However, there are boundary layers, such as upwelling layers, in which the balance is *not* geostrophic for both components (see e.g. GILL and CLARKE, 1974). In these layers, the flow parallel to the coast is balanced by a pressure gradient, but for the flow normal to the coast, the other terms in (3.1) or (3.2) are of the same order. Thus the 'quasi-geostrophic' approximation does not correctly describe the relation between velocity and pressure in such regions, but the above relations do. An approximation of the above type was suggested by FJORTOFT (1962).

If (3.1) and (3.2) are substituted in (2.3), a single equation for the pressure results, namely

$$\left[\left(\frac{\cos\theta\, p_\theta}{R^2\sin^2\theta}\right)_\theta + \frac{\sec\theta}{R^2\sin^2\theta}p_{\lambda\lambda} - \cos\theta\left(\frac{2\Omega}{c}\right)^2 p\right]_t + \frac{2\Omega\cos\theta}{R^2\sin^2\theta}p_\lambda = \frac{2\Omega}{RH}\left[\frac{\tau^y_\lambda}{\sin\theta} - \left(\frac{\tau^x\cos\theta}{\sin\theta}\right)_\theta\right]. \quad (3.3)$$

4. THE BETA-PLANE APPROXIMATION

When the latitude θ does not depart too much from a given latitude θ_0, equation (3.3) is often approximated by an equation with constant coefficients, namely

$$\left(p_{xx} + p_{yy} - \frac{f^2}{c^2}p\right)_t + \beta\, p_x = -\frac{f}{H}\left(\tau^x_y - \tau^y_x\right), \quad (4.1)$$

which is called the beta-plane approximation to (3.3). In this equation

$$x = R\cos\theta_0\lambda \qquad y = R(\theta - \theta_0)$$
$$f = 2\Omega\sin\theta_0 \qquad \beta = 2\Omega\cos\theta_0/R.$$

In order to calculate velocities as well as pressures, it is desirable to have also approximations to (3.1), (3.2) and (2.3) which (i) are consistent with (4.1), (ii) have constant coefficients and (iii) are valid in upwelling layers. For this purpose, first define

$$p^* = \frac{\sin\theta_0}{\sin\theta}p.$$

Then (3.1) and (3.2) become

$$fu = -\frac{1}{R}p^*_\theta - \frac{\cot\theta}{R}p^* - \frac{\sec\theta}{2\Omega R\sin\theta}p^*_{\lambda t} + \frac{\tau^y\sin\theta_0}{H\sin\theta}$$

$$fv = \frac{1}{R}\sec\theta\, p^*_\lambda - \frac{1}{2\Omega R\sin^2\theta}(p^*\sin\theta)_{\theta t} - \frac{\tau^x\sin\theta_0}{H\sin\theta}.$$

The beta-plane approximation to these equations which has the desired properties, is, after dropping the asterisks

$$fu = -p_y - \frac{\beta}{f}p - \frac{1}{f}p_{xt} + \frac{\tau^y}{H} \quad (4.2)$$

$$fv = p_x - \frac{1}{f}p_{yt} - \frac{\tau^x}{H}. \quad (4.3)$$

The beta-plane approximation to (2.3) is

$$p_t + c^2(u_x + v_y) = 0. \quad (4.4)$$

It can be seen that (4.1) is obtained when u and v are eliminated from (4.2), (4.3) and (4.4).

5. METHOD OF SOLUTION

The aim is to show how the interior and the eastern and western boundary layers develop when a wind stress is suddenly applied to the ocean. To illustrate what happens, a simple geometry has been chosen, namely an ocean contained between two meridional boundaries $x = -L$ and $x = L$, and periodic behaviour with y is assumed. The wind stress is usually taken to be independent of x, and since the system is linear, results for an east–west stress τ^x can be discussed separately from those for a north–south wind stress. The former case will be discussed here and in Sections 6 to 8, and the latter in Sections 9 and 10.

Because of the periodic behaviour in y, the operator $\partial/\partial y$ can be replaced by il where l is the north–south wavenumber. Then (4.2) may be

written

$$fu = -l(i + \varepsilon)p - \frac{1}{f}p_{xt} + \frac{\tau^y}{H}, \tag{5.1}$$

where $$\varepsilon = \beta/fl \tag{5.2}$$

is a small non-dimensional parameter. In fact, the β-plane approximation is based on the assumption that ε is small. Now, applying the operator

$$-l(i + \varepsilon)/f - \frac{1}{f^2}\frac{\partial^2}{\partial x \partial t}$$

to (4.1), an equation for u results, namely

$$(u_{xx} - \mu^2 u)_t + \beta u_x = -\frac{l^2}{H}(1 - i\varepsilon)\tau^x, \tag{5.3}$$

where $$\mu^2 = \left(\frac{f}{c}\right)^2 + l^2 \quad . \tag{5.4}$$

Solution of (5.4) by a time-stepping technique is now straightforward, since the boundary conditions at $x = -L$, L are such that u is zero. It is important to use a numerical scheme which adequately represents propagating waves, so a spectral method was used, variables being expanded as a series of Chebyshev polynomials (FOX and PARKER, 1968, Chapter 3). These give higher resolution in the boundary layers, and, as confirmed by trial and error, require fewer terms for given accuracy than a Fourier series (see ORSZAG, 1971). As time goes on, the western boundary layer becomes steadily thinner (LIGHTHILL, 1969, 1971), so the number of terms required in the Chebyshev expansion is determined by the length of time for which an accurate solution is needed.

The solutions of (5.4) depend on only one non-dimensional parameter,

$$\Lambda = \mu^2 L^2. \tag{5.5}$$

For the barotropic mode, $\mu^{-1} \sim l^{-1} \sim 1000$ km, so if $L \sim 3000$ km, Λ is about 10. On the other hand, for a baroclinic mode, $\mu^{-1} \sim c/f$, i.e. the baroclinic radius of deformation, which is typically 30 km. For this mode Λ is of order 10,000. To calculate solutions for such a large value would require a very large number of terms in the Chebyshev expansion. Since it is unnecessary to have such a large value in order to illustrate the behaviour of the solution, more modest values were used, the largest being 600.

6. RESULTS FOR AN EAST–WEST WIND STRESS

PEDLOSKY (1965a, b) and PHILLIPS (1966) have discussed periodic solutions to this problem, but the spin-up effect resulting from an impulsively applied wind stress has not received so much attention. LIGHTHILL (1969) has discussed various aspects of this problem and in particular the behaviour of the western boundary layer. Lighthill showed how the solution can be found by a transform method, which is equivalent to integrating a set of periodic solutions. Thus some properties of the solution can be deduced from the properties of wave-like disturbances. The wave-like solutions are of two types (YOSHIDA, 1960; FOFONOFF, 1962), called Rossby or planetary waves (which have frequencies less than $\beta/2\mu$) and Kelvin waves which have frequencies greater than $\beta/2\mu$.

Before discussing the solution further, it is convenient to put (5.3) in non-dimensional form by using L as a scale for x, $(\beta L)^{-1}$ as a scale for t and $Ll^2(1 - i\varepsilon)\tau^x/\beta H$ as a scale for u. Then (5.3) becomes

$$(u_{xx} - \Lambda u)_t + u_x = 1, \tag{6.4}$$

where

$$\Lambda^{\frac{1}{2}} = (l^2 + a^2)^{\frac{1}{2}}L \quad (a = f/c) \tag{6.5}$$

is the ratio of the natural scale $(l^2 + a^2)^{-\frac{1}{2}}$ of the problem to the scale of the basin. The boundary conditions are

$$u = 0 \text{ at } x = \pm 1. \tag{6.6}$$

The solutions of (6.4) can be expressed as the sum of a particular solution, and a solution of the homogeneous equation. The particular solution can be chosen as either the time-independent solution which satisfies

$$u_x = 1 \tag{6.7}$$

or as the space-independent solution

$$u = -t/\Lambda. \tag{6.8}$$

The former solution is Sverdrup's solution, whilst the latter is the solution which applies in the absence of boundary effects. To take account of initial and boundary conditions, a solution of the homogeneous equation

$$(u_{xx} - \Lambda u)_t + u_x = 0 \tag{6.9}$$

must be added. This is the familiar planetary wave equation. Boundary effects propagated by these waves have a group velocity (LONGUET-HIGGINS, 1965) given by

$$C_g = \frac{k^2 - \Lambda}{(k^2 + \Lambda)^2}. \tag{6.10}$$

The largest group velocity occurs at $k = 0$ when $C_g = -1/\Lambda$. As k increases, C_g changes sign and increases to a value of $1/8\Lambda$ at $k = \sqrt{3\Lambda}$ and then falls to zero as $k \to \infty$. Thus information from the eastern boundary is rapidly transmitted westwards by the longest waves, while information from the western boundary can be transmitted eastwards at only one-eighth of the speed by relatively short waves. Thus the solution has a different character in three different regions. In the interior region, i.e. the region where boundary effects have not yet been felt, the solution is given by (6.8). This interior region is bounded by two moving boundaries. The one to the west moving eastwards at a speed of $1/8\Lambda$ and the one to the east moving westwards at a speed of $1/\Lambda$. The latter front is due to long waves propagating energy westwards, and so the solution on either side is dominated by the long wave solution [for which the term u_{xxt} in (6.4) and (6.9) is negligible]. Thus the solution to the east of the front is approximately equal to Sverdrup's solution

$$u = x - 1. \tag{6.11}$$

The solution near the western boundary will be discussed in the next section.

7. THE WESTERN BOUNDARY LAYER

As time goes on, the solution near the western boundary will be increasingly dominated by short waves, as these propagate information eastwards only very slowly. The short-wave approximation to (6.4) is

$$u_{xxt} + u_x = 0, \tag{7.1}$$

where in the western boundary layer, u is required to vanish at $x = -1$ and to match with the appropriate interior solution valid outside the boundary-layer. Equation (7.1) has the set of similarity solutions

$$\left(\frac{t}{1+x}\right)^{\nu/2} J_\nu\,[2\sqrt{(1+x)t}], \tag{7.2}$$

where ν is a constant and J_ν is the Bessel function of order ν. When (6.8) is the appropriate interior solution, the appropriate value of ν is 1 and the solution of (7.1) matching this interior solution is

$$u = -\frac{1}{\Lambda}\left\{t - \left(\frac{t}{1+x}\right)^{\frac{1}{2}} J_1[2\sqrt{(1+x)t}]\right\}. \tag{7.3}$$

In Fig. 1, this solution is plotted as a function of x for various values of t, for the case $\Lambda = 600$. The value of Λ is somewhat less than would be appropriate for the baroclinic modes, but is sufficiently large to separate the boundary flow from the Sverdrup flow for sufficiently long a time for a solution of the form (7.3) to be established and consequently little extra insight would be obtained by using a larger value of Λ.

In Fig. 2 is shown the solution computed from (6.4) for the above value of Λ. The agreement in the western region is good, confirming the above ideas. The interior increasing linearly with t up to a time comparable with the time it takes a long planetary wave to propagate from the eastern boundary is clearly visible. In the

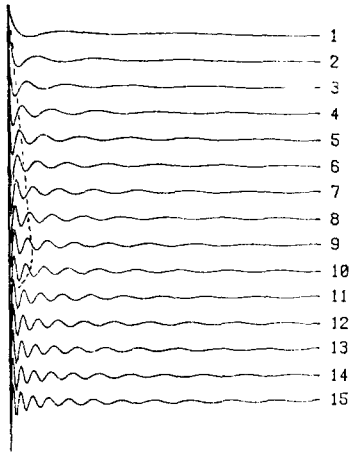

Fig. 1. Plot of (7.3) as a function of x for various values of t. The value of Λ is 600. The region to the left of the dashed line is that in which the above function is a good approximation to the numerically determined solution of (6.4). The plotting frequency is 100 units of dimensionless time.

wake of this planetary wave, the solution is closely approximated by the Sverdrup solution, $u = x - 1$, though there are perturbations on this basic flow. Results to be discussed later show that the amplitude of these perturbations increases as Λ decreases.

There are two limitations on the validity of (7.3). Firstly it cannot be valid for times longer than 2Λ since by then the interior solution, where it matches with (7.3), is changing from the growing solution (6.8) to the Sverdrup solution (6.11). Secondly, the western boundary can only affect the solution a finite distance, d_w, from the western boundary. This distance is made up of two parts. The first is the maximum distance $t/8\Lambda$ (see Section 6) to which affects can be carried by planetary waves. The second distance δ is the one which results from making the system 'incompressible' to inertial-gravity waves. This distance is the trapping scale

$$\delta \sim \Lambda^{-\frac{1}{3}} \tag{7.4}$$

of the solutions of (6.4) with exponential character and is approximately equal (see Section 5) to the baroclinic radius of deformation in the case of the baroclinic mode. Thus

$$d_w = \delta + t/8\Lambda. \tag{7.5}$$

Since (7.1) is valid only for scales small compared with δ, (7.3) will only be valid for distances from the boundary less than δ. However, consideration of the solution obtained by transform methods (cf. LIGHTHILL, 1969, p. 62) shows that an improved approximation is given by

$$u = -\frac{1}{\Lambda}\left(t - \left(\frac{t}{1+x}\right)^{\frac{1}{2}} J_1\{2\sqrt{(1+x)[t - \Lambda(1+x)]}\}\right). \tag{7.6}$$

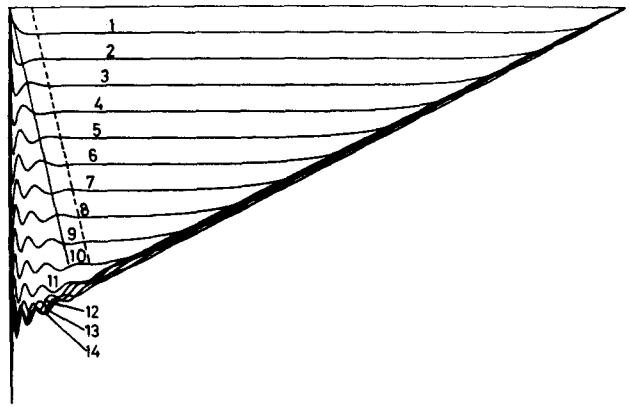

Fig. 2. The numerically determined solution of (6.4) for comparison with Fig. 1. The solid diagonal line denotes the maximum distance information from the western boundary could have been propagated eastward into the interior by planetary waves. The dashed line is displaced a distance δ from the solid line.

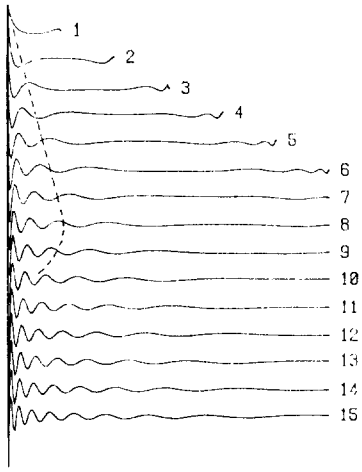

Fig. 3. Plot of (7.6) for comparison with Figs. 1 and 2. The region to the left of the dashed line is that in which the above function is a good approximation to that of Fig. 2.

This solution is shown in Fig. 3 and is in excellent agreement with the exact solution right up to a distance d_w from the western boundary.

A noticeable difference between Figs. 1 and 3 is in the position of maxima and minima of u. In the approximation (7.3), their position is given by

$$1 + x = b_n t^{-1}, \tag{7.7}$$

where $$b_n = (\tfrac{1}{2} j_{2,n})^2, \tag{7.8}$$

and $j_{\nu,n}$ is the nth zero of the Bessel function J_ν of order ν. Thus $b_1 = 6{\cdot}6$ (ABRAMOWITZ and STEGUN, 1965). In the improved approximation (7.6), the maxima and minima are moved a little further out, to the positions given by

$$1 + x \doteq b_n t^{-1}(1 + \Lambda b_n t^{-2}). \tag{7.9}$$

For times greater than 2Λ, the Sverdrup solution (6.11) is established in the whole of the interior, so the western boundary-layer solution must match (6.11). The solution (LIGHTHILL, 1969) equivalent to (7.6) is

$$u = 2J_0\{2\sqrt{(1 + x)[t - \Lambda(1 + x)]}\} - 1 + x. \tag{7.10}$$

The maxima and minima are again at points given by (7.9), but now with

$$b_n = (\tfrac{1}{2} j_{1,n})^2, \tag{7.11}$$

so $b_1 = 3{\cdot}7$ is now smaller. The values of u at the extrema are approximately

$$u_n = 2J_0(j_{1,n}) - 2, \tag{7.12}$$

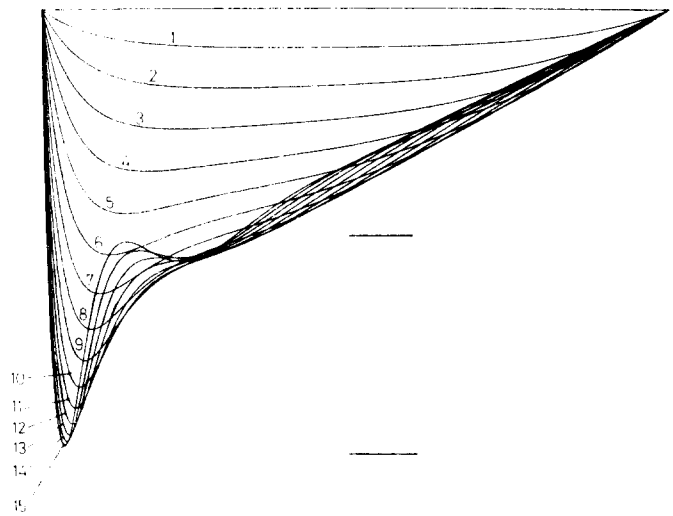

Fig. 4. Numerically determined solution of (6.4) for $\Lambda = 20$. There is no obvious J_1 spin-up solution for this case because the Sverdrup solution is established across the whole ocean before such a boundary layer can become well established. The J_0 solution which occurs for large time is apparent, however. Solid horizontal lines are at $u = -2{\cdot}8$, and $u = -1{\cdot}4$. The plotting frequency is 5 units of dimensionless time.

so $u_1 = 2{\cdot}8$ and $u_2 \doteq -1{\cdot}4$.

To test these ideas, results were computed for $\Lambda = 20$, the curves obtained being shown in Fig. 4. The positions of the first maximum and minimum are satisfactorily predicted by the above formulae. The value of u at the first minimum is close to u_1 at large times. The value at the first maximum is reasonably close to u_2, but more variable with time. By way of comparison, Figs. 5a and 5b show results for a relatively small value, $\Lambda = 4$, which corresponds to a barotropic wave. The most noticeable difference with this case is that large oscillations extend over most of the basin, although still decreasing toward the east. For even smaller Λ, this oscillation can actually make u reverse near the eastern boundary. This reversal is associated with the arrival at the eastern boundary of short planetary waves from the western boundary.

8. FORCING CONFINED TO ONLY PART OF THE BASIN

In this section, the barotropic flow resulting from the application of a steady wind stress curl in a region remote from the western boundary is examined. LIGHTHILL (1969) considered a problem of this type in order to calculate changes in the Somali Current resulting from the onset of the Southwest Monsoon in a region remote from the current. Lighthill's results suggest a J_0 type of response in the western boundary, rather independent of the actual form of remote forcing.

The results of the computations are shown in Fig. 6. The value $\Lambda = 20$ was chosen as the results are only considered applicable to the barotropic mode in low latitudes. The equation is

$$(u_{xx} - \Lambda u)_t + u_x = \begin{cases} 1 \text{ for } x > 0 \\ 0 \text{ for } x < 0 \end{cases}, \tag{8.1}$$

i.e. the forcing is confined to the eastern half of the basin, where it is uniform.

The calculated solutions may be compared with the long-wave solution of (8.1), i.e. the one obtained by ignoring the term u_{xxt}. For $t < \Lambda$, this solution is

$$\begin{aligned} u &= x - 1 && \text{for} && x > 1 - t/\Lambda \\ u &= -t/\Lambda && \text{for} && 0 < x < 1 - t/\Lambda \\ u &= -x - t/\Lambda && \text{for} && 0 > x > -t/\Lambda \\ u &= 0 && \text{for} && x < -t/\Lambda. \end{aligned} \tag{8.2}$$

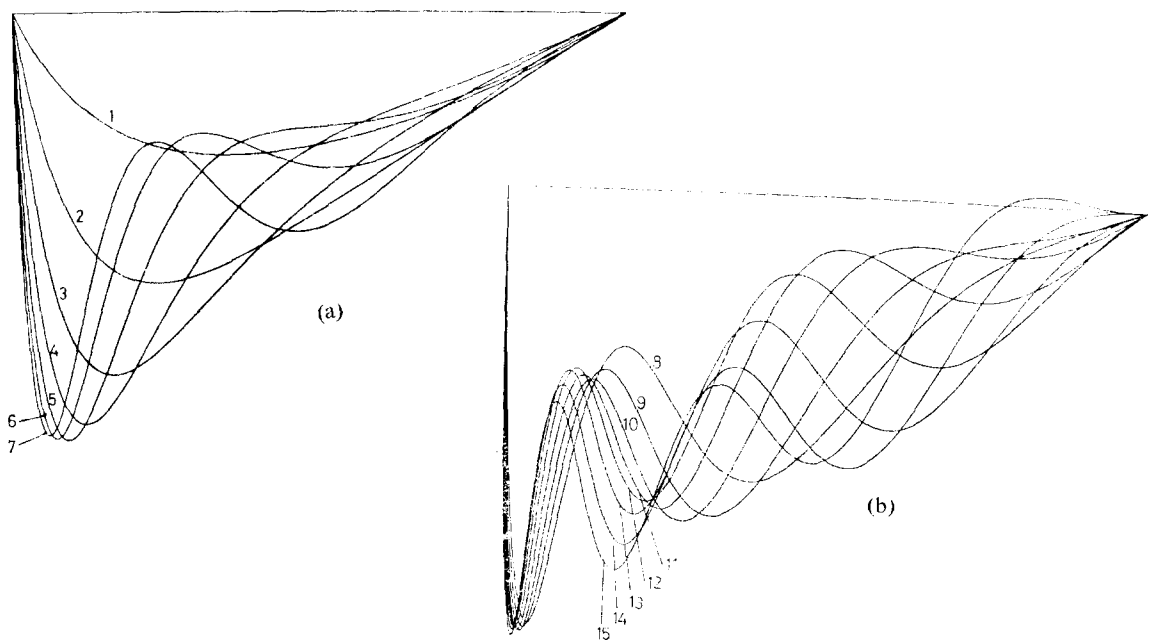

Fig. 5a, b. As for Figs. 2, 4 but for $\Lambda = 4$. Note the larger amplitude perturbations across the whole width of the basin. Curves plotted every 5 units of dimensionless time.

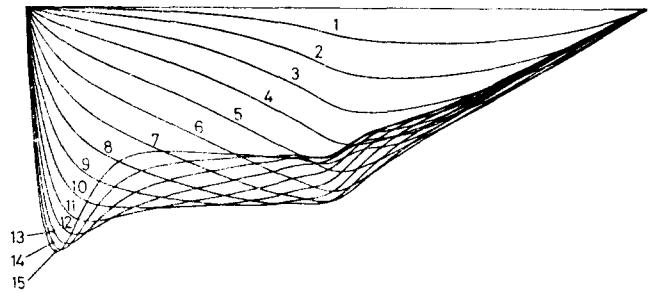

Fig. 6. Time evolution of the barotropic flow for $\Lambda = 20$ when a unit wind stress is applied in the region $0 < x < 1$ only. In this region the Sverdrup flow is $u_x = 1$; for $-1 < x < 0$, it is $u = -1$, modulated near the western boundary by a J_0 type boundary layer. Note the rapid spin-up of the interior flow in the region where there is no local forcing. Compare with Fig. 4 which is for unit forcing over the whole basin $-1 < x < 1$.

For $t > \Lambda$, the long-wave solution is

$$\begin{aligned} u &= x - 1 \quad \text{for} \quad x > 0 \\ u &= -1 \quad \text{for} \quad x > 1 - t/\Lambda \\ u &= -x - t/\Lambda \quad \text{for} \quad x < 1 - t/\Lambda. \end{aligned} \tag{8.3}$$

The long-wave solution describes the gross features of the solution, but there are noteworthy differences. For instance, there is an instantaneous response all over the western half of the basin despite the fact that no planetary wave can have penetrated this region completely. This is due to the exponentially decaying solutions of (6.9). The instantaneous response is due to filtering out inertial-gravity waves, the approximation effectively giving these waves infinite propagation speed.

The development of the western boundary layer can be discussed as in the last section. After the Sverdrup interior has been established ($t \approx 2\Lambda$), the western boundary layer solution is approximately given by (7.10), but with the last term ($+x$) removed and the coefficient of J_0 reduced to unity. This predicts the first minimum of u as being $-1{\cdot}4$ in agreement with the numerically obtained value (Fig. 6).

9. FORCING BY A NORTH–SOUTH WIND STRESS

In this section, the solution for a north–south wind stress that varies sinusoidally with y will be derived. The equation for u is (5.3), except that in this case the right-hand side vanishes for $t > 0$. If the effect of the impulsive application of the wind stress at $t = 0$ is included, the right-hand side becomes

$$-\frac{\mu^2 \tau^y}{f\ H}\,\delta(t).$$

The solution when β-plane dynamics are excluded, i.e. the f-plane solution, is familiar from the work of CHARNEY (1955). This solution is given by

$$u = -\frac{\tau^y}{fH}\left(\frac{\cosh \mu x}{\cosh \mu L} - 1\right), \tag{9.1}$$

where μ is defined by (5.4). For the baroclinic case where μL is large, u is constant except near the boundaries, the value of the constant being the contribution to the baroclinic mode from the Ekman flux. Near each coastline, there is a narrow boundary layer of thickness μ^{-1} in which u falls to zero. The associated divergence requires movement of the thermocline so this narrow region is characterized by upwelling and a longshore coastal jet associated geostrophically with the thermocline slope. Note that the u-field is set up instantaneously, a result of making the medium 'incompressible' to inertial-gravity waves. The solution has the trapping scale (7.4) associated with this approximation as noted before.

Now consider the β-plane solution for u. Choosing τ^y/fH as a scale for u and the same x and t scales as before [L and $(\beta L)^{-1}$, respectively], the equation for u becomes, for $t > 0$,

$$(u_{xx} - \Lambda u)_t + u_x = 0. \tag{9.2}$$

The initial condition is that u is the same as the f-plane solution which is impulsively generated at $t = 0$, i.e.

$$u = 1 - \frac{\cosh \sqrt{\Lambda}\, x}{\cosh \sqrt{\Lambda}} \quad . \tag{9.3}$$

The presence of planetary waves on the β-plane changes the nature of the solution only slightly for short times, but makes a profound difference for the longer term solution. This is because planetary waves allow energy to leak westwards, so it is no longer trapped within a Rossby radius of deformation of the coast as it is on an f-plane. To assess the leakage of energy from the f-plane solution to the west, (9.2) has been solved numerically by the same methods as outlined in previous sections. The solution for $\Lambda = 600$ is shown in Fig. 7.

By arguments similar to those of Section 6, one would expect the interior solution to remain at the initial value $u = 1$ until the arrival of planetary waves from the boundaries, the fastest ones being the long waves from the east. After the passage of these waves, the solution should asymptote to $u = 0$, the Sverdrup solution. Figure 7 shows that such is indeed the case. Of interest here is the wave-like wake left behind after the passage of the primary front. For given t, the variations with respect to x show a primary wave followed by a succession of other waves. The number of waves increases with t, but the amplitude and wavelength decrease with x. At any given x, the flow not only relaxes to zero, but in fact changes sign for a time, i.e. the solution overshoots the asymptotic limit. The time taken for the u-field to change significantly is of order $\Lambda^{\frac{1}{2}}$, e.g. the value of u_x at the eastern boundary first falls to zero at $t = 4\Lambda^{\frac{1}{2}}$, i.e. about

$$4\mu/\beta \approx 4f/\beta c \tag{9.4}$$

units of real time. For $f/\beta \sim 5000$ km, $c \sim 2{\cdot}5\,\mathrm{m\,s^{-1}}$ this is about 3 months. The implication is that on times small compared with this, the upwelling associated with cyclone-scale forcing will be largely unaffected by the β-effect and that coastal Kelvin wave solutions for such frequencies may be sought on an f-plane (GILL and CLARKE, 1974). However, upwelling on a seasonal time scale will be considerably influenced by this process, so computations of such longer term changes must contain β-plane dynamics (WHITE and MCCREARY, 1974).

Near the western boundary, the solution will be determined by the boundary-layer equation (7.1) whose solutions have already been given in Section 7. The solution appropriate for the case in hand is

$$u = (1 - J_0\{2\sqrt{(1+x)}\,[t - \Lambda(1+x)]\}), \tag{9.5}$$

for values of t less than 2Λ, the time for the planetary waves from the east to reach the western boundary. The development of the solution with this character near the western boundary can be seen in Fig. 7.

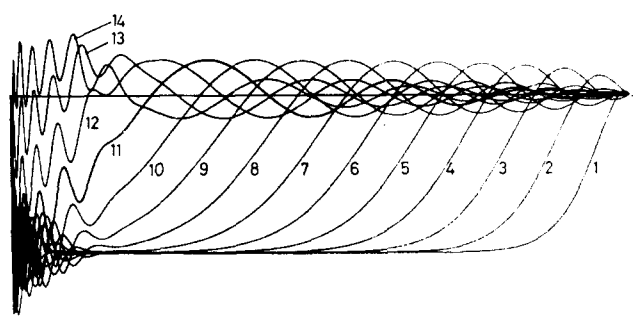

Fig. 7. Relaxation of the f-plane solution (9.3) for a steady longshore wind stress independent of x, y when β effects are included (9.2). The propagation of Rossby waves from the east is clearly visible. The solution relaxes to the Sverdrup solution $u = 0$. Curves are plotted every 100 units of dimensionless time.

An interesting comparison between the f-plane and the β-plane solutions is in the nature of the interior solution after a long time. In the f-plane solution, this consists of the Ekman flux in the top layer. In the β-plane solution, there is no net flow so the Ekman flux in the top layer is balanced by a geostrophic flow in the opposite direction, also within the top layer. The geostrophic flow must be associated with a north–south pressure gradient established after the passage of the planetary waves. The comparison of the f-plane and β-plane solutions for the pressure will be made in the next section.

10. SOLUTION FOR THE THERMOCLINE DISPLACEMENT

In the last section, the solution was found for the eastward-velocity component u. In this section, the corresponding solution for the pressure p will be discussed. For a two-layer model with a deep lower layer, the thermocline displacement h is given by

$$h \sim p/g'\rho. \tag{10.1}$$

The solution for p must satisfy (4.2) and also the equation obtained by substituting (4.3) for v in (4.4). For the f-plane case, this solution can be obtained analytically. The result, which can be confirmed by substitution, is

$$p = \frac{\tau^y}{lH \cosh \mu L}\left[\sinh \mu x \sin \frac{flt}{\mu} + \right.$$
$$\left. + i \cosh \mu x \left(\cos \frac{flt}{\mu} - 1\right)\right]. \tag{10.2}$$

For the baroclinic mode, for which μL is large, this solution is only significant in the coastal boundary layers. Near the eastern boundary, if the $\exp(ily)$ factor is included and the real part taken, (10.2) gives

$$p = (\tau^y/lH)\, e^{\mu(x-L)} [\sin ly -$$
$$- \sin l(y - ft/\mu)], \tag{10.3}$$

i.e. is the sum of a stationary forced solution and a northward (in the northern hemisphere) travelling Kelvin wave. Initially the two sinusoids cancel so p is zero, but then p increases linearly with time as the two sinusoids get out of phase. Eventually $|p|$ reaches a maximum value of

$$p_{\max} = 2\tau^y/lH, \tag{10.4}$$

which is achieved at intervals of

$$\pi\mu/fl \sim \pi/cl$$

as successive waves pass by along the coast.

Note that the time-averaged value of p is a maximum at $y = \pi/2l$, whereas the wind is a maximum at $y = 0$. In other words, the maximum average upwelling is a quarter of a wavelength poleward of the maximum equatorward wind.

The following discussion is about the baroclinic mode, so it is assumed that μL is large and $\mu \sim f/c$. Then for the β-plane model, two time scales enter the problem. These are the time scale $(cl)^{-1}$ of the Kelvin waves, which appears in (10.3) and the time scale $f/\beta c$ (see Section 9) for planetary wave effects to influence the eastern boundary layer. The ratio of the two time scales is

$$\varepsilon = \beta/fl \quad ,$$

(see 5.2) which is normally small, so the time scale for planetary wave effects to take place is longer. From dimensional arguments, (10.3) will be valid for a time comparable with that given by (9.4), but dimensional arguments can give no information about the actual numerical coefficients. For a more quantitative estimate, the solution for p at the eastern boundary is required. The solution, found by Laplace transform methods, is

$$\frac{\beta Hp}{f\tau} = \frac{1}{1 + i/\varepsilon} - \frac{2i}{\pi}\int_1^\infty \cos\left(\frac{\beta ct}{2f} R\right)$$
$$\left[\left(1 + \frac{2i}{\varepsilon} - i\sqrt{R^2 - 1}\right)^{-1} - \right.$$
$$\left. \left(1 + \frac{2i}{\varepsilon} + i\sqrt{R^2 - 1}\right)^{-1}\right] dR. \tag{10.5}$$

This solution should be contrasted with (10.2). Firstly, it is not obvious that the Kelvin wave frequency (cl) is present in (10.5). However, it can be shown that in the limit $\varepsilon \to 0$ with $flt/\mu \approx clt$ fixed, (10.5) tends to the value given by (10.2) at the eastern boundary $x = L$.

Figure 8 shows the behaviour of the imaginary part of (10.5) for several values of ε and $\Lambda = 150$. For small ε, it is clear that the oscillation suffers severe damping in the time scale given by (9.4) as suggested above, but even for times as small as $f/\beta c$ the oscillation is damped by nearly 50%, suggesting that (9.4) is an overestimate of the

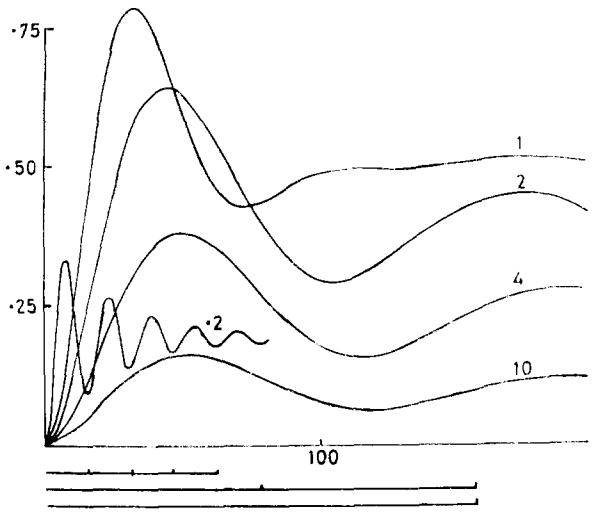

Fig. 8. Plot of the imaginary part of (10.5) for $\Lambda = 150$ as a function of dimensionless time for the values of $\varepsilon = 0{\cdot}2, 1, 2, 4, 10$. Damped oscillations are evident for all values of ε, but only for the smallest value of ε does the period of the oscillation match the Kelvin wave period $2\pi\sqrt{\Lambda\varepsilon}$, indicated by the solid lines at foot of graph for $\varepsilon = 0{\cdot}2, 1, 2$.

time scale on which β-effects modify upwelling. For times longer than $f/\beta c$ the integral in (10.5) becomes small, and p tends to a steady value. Planetary waves carry the upwelling westward and in a steadily widening zone, upwelling of amplitude $\frac{f\tau}{\beta H}(1 + i/\varepsilon)^{-1}$ results. This effect is shown in Fig. 9, in which the imaginary part of p is plotted as a function of x for various values of dimensionless time for $\Lambda = 150$.

If $l = 10^{-6}$ m^{-1}, $\tau = 0{\cdot}1$ N m^{-2}, and

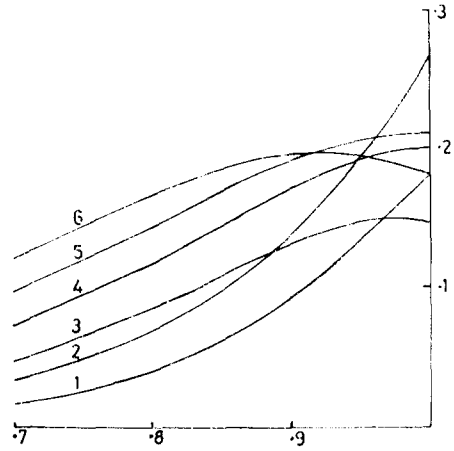

Fig. 9. Plot of the imaginary part of $\beta Hp/f\tau$ as a function of x away from the eastern boundary for $\Lambda = 150$, $\varepsilon = 0{\cdot}2$. The curves are plotted every 10 units of dimensionless time. The width of the upwelling zone can be seen to broaden with time and to asymptote to a value $\varepsilon/(1 + \varepsilon^2)$.

$g' = 0{\cdot}03$ m s^{-2}, (10.1) and (10.5) give a mean displacement of 3000/H m^{-1}. This is only 6 m for a normal thermocline depth of 500 m, but in upwelling areas a more appropriate value of H is 100 m in which case the displacement is 30 m. The time required to damp the oscillations by 50% is about a month if f/β and c have the values in Section 9.

There is also some interest in the limit $\varepsilon \to \infty$, corresponding to no longshore variation, as the f-plane solution for this case is often quoted. In this case, p grows linearly with time in the f-plane case but tends to a limit of (see 10.6)

$$p = f\tau/\beta H$$

in the β-plane case, this limit being achieved in the time scale given by (9.4). In this limit, the maximum upwelling occurs where the wind is a maximum.

HULBURT and THOMPSON (1973) made numerical studies for the case $l = 0$ ($\varepsilon = \infty$) in order to compare f-plane and β-plane models. Their forcing lasted for 15 days, for which β-effects are very important for the barotropic mode but of little significance for the baroclinic mode. This is presumably the reason why they found a poleward undercurrent only in the β-plane case, although the thermocline displacement was much

the same in the two cases. Hurlburt and Thompson continued their calculation after the forcing was turned off, and the widening of the upwelling zone due to β-effects is visible in Fig. 8 (corresponding to day 50) of their paper.

The differences between f-plane and β-plane solutions for large ε are of somewhat academic interest in that the β-plane approximation, as normally derived, is based on the assumption that ε is small. Even when ε is small, the β-plane (and f-plane) solution for p only approximates to the solution on a *spherical Earth* for a limited time. This is because Kelvin waves propagate information from one latitude to another (with appreciably different values of β and f) in a time of order R/c, where R is the radius of the Earth. In fact, Kelvin waves take this order of time to propagate from the equator where they may have been produced by interaction of an equatorial Kelvin wave with the coast. Since R/c is of the same order as (9.4), the solutions given in this section show the *nature* of β-effects on upwelling, but accurate solutions for a spherical Earth would require a more careful analysis. Of course, planetary wave propagation is only one of many effects which are likely to be important in practice, and this section aims merely to clarify the nature of the one effect.

11. SUMMARY

The response to an applied wind stress of a two-layer ocean is examined. The ocean is on a β-plane, is contained between rigid north–south boundaries and has fixed stratification. For steady east–west wind stress, it is found that during spin-up, the baroclinic flow in the interior increases linearly with time, until a non-dispersive Rossby wave has time to propagate from the eastern boundary. The flow behind this wave is then of the Sverdrup type. Near the western boundary, the flow builds up linearly with time also, but with a perturbation of the form $J_1[2\sqrt{(1+x)t}]/\sqrt{(1+x)t}$ superimposed, which leads to a thinning boundary layer. After a time sufficiently long for the westward travelling wave to cross the whole basin, the flow near the western boundary changes to a steady flow with perturbations of the form $J_0[2\sqrt{(1+x)t}]$. The perturbations are of larger amplitude in this latter state but the rate of thinning is reduced.

For the case of steady longshore wind stress, a comparison is made between the solution obtained for f-plane dynamics and that for β-plane dynamics. For both cases, the offshore velocity u is unperturbed by coastal Kelvin waves and thus a comparison can be made between the two solutions which is independent of l. On the β-plane, planetary waves allow the eastern boundary initially of width c/f to broaden and for u to relax to zero. During the course of this relaxation, the velocity can undergo a complete reversal, implying that the Ekman flux can be more than offset by reverse flow below the Ekman layer but above the main thermocline.

On the f-plane, for a wind stress sinusoidal in y, upwelling is in the mean located not at the position of maximum equatorward wind stress but a quarter wavelength poleward. This result is a consequence of coastal Kelvin waves carrying energy polewards. Because the pressure field is sensitive to Kelvin waves, a comparison between the β-plane and f-plane solution is dependent on l. The maximum difference occurs when $l = 0$: on the f-plane the upwelling increases linearly with time whereas on the β-plane upwelling can attain a maximum value $f\tau/\beta H$. As l is increased the mean β-plane solution approaches the mean f-plane solution near the coast and again suffers a phase shift. On the f-plane, Kelvin waves are unattenuated but they are damped on the β-plane. Also, on the β-plane upwelling is not restricted to the coastal region but can propagate westwards.

REFERENCES

ABRAMOWITZ M. and I. A. STEGUN (1965) *Handbook of mathematical functions*, Dover, 1046 pp.

CHARNEY J. G. (1955) The generation of oceanic currents by wind. *Journal of Marine Research*, **14**, 477–498.

FJORTOFT R. (1962) On the integration of a system of geostrophically balanced prognostic equations. *Proceedings of the International Symposium on Numerical Weather Prediction*. Meteorological Society of Japan, Tokyo, pp. 153–159.

FOFONOFF N. P. (1962) Dynamics of ocean currents In: *The sea*, M. N. HILL, editor, Interscience, Vol. 1, pp. 323–380.

FOX L. and I. B. PARKER (1968) *Chebyshev polynomials in numerical analysis*, Oxford University Press, 205 pp.

GATES W. L. (1968) A numerical study of transient Rossby waves in a wind-driven homogeneous ocean. *Journal of the Atmospheric Sciences*, **25**, 3–22.

GILL A. E. and A. J. CLARKE (1974) Wind-induced upwelling, coastal currents and sea-level changes. *Deep-Sea Research*, **21**, 325–345.

HURLBURT H. E. and J. D. THOMSON (1973) Coastal upwelling on a β-plane. *Journal of Physical Oceanography*, **3**, 16–32.

ICHIYE T. (1972) A theory of coastal upwelling based on a two-layer ocean model and its application to the eastern Pacific Ocean. IV *Congreso Nacional de Oceanografia, Memorias, Mexico*, pp. 13–36.

LIGHTHILL M. J. (1969) Dynamic response of the Indian Ocean to onset of the Southwest Monsoon. *Philosophical Transactions of the Royal Society of London*, **A265**, 45–92.

LIGHTHILL M. J. (1971) Time varying currents. *Philosophical Transactions of the Royal Society of London*, **A270**, 371–390.

LONGUET-HIGGINS M. S. (1965) The response of a stratified ocean to stationary or moving wind systems. *Deep-Sea Research*, **12**, 923–973.

ORSZAG S. A. (1971) Galerkin approximations to flows within slabs, spheres and cylinders. *Physical Review Letters*, **26**, 1100–1103.

PEDLOSKY J. (1965a) A study of the time-dependent ocean circulation. *Journal of the Atmospheric Sciences*, **22**, 267–272.

PEDLOSKY J. (1965b) A note on the western intensification of the oceanic circulation. *Journal of Marine Research*, **23**, 207–209.

PEDLOSKY J. (1967) Fluctuating winds and the ocean circulation. *Tellus*, **19**, 250–257.

PHILLIPS N. A. (1966) Large-scale eddy motion in the western Atlantic. *Journal of Geophysical Research*, **71**, 3883–3891.

VERONIS G. (1963) An analysis of wind-driven ocean circulation with a limited number of Fourier components. *Journal of the Atmospheric Sciences*, **20**, 577–593.

VERONIS G. (1966) Generation of mean ocean circulation by fluctuating winds. *Tellus*, **18**, 67–76.

VERONIS G. (1970) Effect of fluctuating winds on ocean circulation. *Deep-Sea Research*, **17**, 421–434.

WHITE W. B. and J. C. MCCREARY (1974) Eastern intensification of ocean spin-down: application to El Niño. *Journal of Physical Oceanography*, **4**, 295–303.

YOSHIDA K. (1960) The oceanic waves of days to months periods. *Records of Oceanographic Works in Japan*, **5**(2), 11–24.